HHS Public Access

Author manuscript

World Neurosurg. Author manuscript; available in PMC 2019 March 01.

Published in final edited form as:

World Neurosurg. 2018 March ; 111: 132–138. doi:10.1016/j.wneu.2017.12.087.

Treatment of progressive herpes zoster-induced vasculopathy with surgical revascularization: effects on cerebral hemodynamics

Sarah K. Lants, BA[a], **Jennifer M. Watchmaker, PhD**[a], **Meher R. Juttukonda, PhD**[a], **Larry T. Davis, MD**[a], **Manus J. Donahue, PhD**[a,b,c,d], and **Matthew R. Fusco, MD**[e]

[a]Department of Radiology and Radiological Sciences, Vanderbilt University Medical Center, Nashville, TN, USA

[b]Department of Psychiatry, Vanderbilt University Medical Center, Nashville, TN, USA

[c]Department of Neurology, Vanderbilt University Medical Center, Nashville, TN, USA

[d]Department of Physics and Astronomy, Vanderbilt University, Nashville, TN, USA

[e]Department of Neurological Surgery, Vanderbilt University Medical Center, Nashville, TN, USA

Abstract

Background—Herpes zoster ophthalmicus (HZO) is caused by the reactivation of the herpes simplex virus in the trigeminal nerve. HZO-initiated cerebral vasculopathy is well-characterized, however there are no documented cases that report the efficacy of surgical revascularization for improving cerebral hemodynamics following progressive HZO-induced vasculopathy. We present a case where quantitative anatomical and hemodynamic imaging were performed longitudinally before and after surgical revascularization in a patient with HZO and vasculopathic changes.

Case Description—A 57-year-old female with history of right-sided HZO presented with left-sided hemiparesis and dysarthria and multiple acute infarcts. Angiography performed serially over a two-month duration revealed progressive middle cerebral artery stenosis, development of new moyamoya-like lenticulostriate collaterals, and evidence of fibromuscular dysplasia in cervical portions of the internal carotid artery. Hemodynamic imaging revealed right hemisphere decreased blood flow and cerebrovascular reserve capacity. In addition to medical therapy, right-sided surgical revascularization was performed with intent to reestablish blood flow. Follow-up imaging 13 months post-revascularization demonstrated improved blood flow and vascular reserve capacity in the operative hemisphere, which paralleled symptom resolution.

Conclusions—HZO can lead to progressive, symptomatic intracranial stenoses. This report suggests that surgical revascularization techniques can improve cerebral hemodynamics and symptomatology in patients with aggressive disease when medical management is unsuccessful;

*Corresponding Author: Sarah K. Lants, Vanderbilt University Medical Center, 1161 21st Ave. South, AA1109, Nashville, TN, 37212, Tel: 615.936.7329, sarah.k.lants@vanderbilt.edu.

similar procedures could be considered in managing HZO patients with advanced or progressive vasculopathy.

Keywords

herpes zoster; moyamoya; stroke; intracranial stenosis; bypass; hemodynamics

Introduction

Herpes zoster ophthalmicus (HZO) results from reactivation of the varicella zoster virus in the ophthalmic segment (V1) of the trigeminal nerve.[1] Severe cases of HZO can result in ipsilateral cerebral angiitis and subsequent cerebral dysfunction.[2] The proposed pathological mechanism is transmission of the virus from the trigeminal nerve to the vessels of the circle of Willis, either via trigeminal branches that innervate the middle cerebral artery (MCA) or direct internal carotid artery (ICA) contact within the cavernous sinus.[3] In cases of HZO-induced vasculopathy, neurological symptoms typically occur at an average of 2-4 months post-infection.[4,5]

Standard treatment options for HZO-related vasculitis are medically-based and focus on anti-inflammatory agents, anti-viral treatment, and support of any underlying vascular insufficiency. However, prolonged or progressive vasculitis may lead to significant arterial steno-occlusion[6] and possible collateral formation in a moyamoya pattern. Medical treatment is unlikely to reverse these end-result changes; thus, surgical revascularization may be considered. The most common type of direct surgical revascularization involves a superficial temporal artery (STA)-to-MCA bypass, which can result in immediate improvement in cerebral blood flow (CBF; ml/100g/min).[7] Indirect revascularization most often involves placement of the STA in proximity to the pia or dura, which leads to neoangiogenesis and enhanced CBF in a delayed fashion through formation of collateral vessels.[7]

We report on a patient with progressive vasculopathy, development of moyamoya collaterals, and multiple progressive ischemic infarcts following HZO infection on standard-of-care medical management. Direct surgical revascularization was performed and the impact of this procedure on cerebral hemodynamics was assessed at multiple time points.

Case report

A 57-year-old Caucasian female with no significant past vascular medical history developed HZO along the right V1 trigeminal nerve distribution. The cutaneous manifestations resolved following treatment with oral valacyclovir. However, two months post-infection she presented to an outside facility with an acute episode of slurred speech and weakness of the left arm, face, and leg, and magnetic resonance imaging (MRI) and computed tomography angiography (CTA) were ordered (Fig. 1). MRI at this time revealed an acute infarct in the right parietal lobe. CTA revealed bilateral carotid fibromuscular dysplasia (FMD) and mild stenosis of the M1 segment of the right MCA and A1 segment of the anterior cerebral artery (Fig. 2A). The patient was discharged after being prescribed clopidogrel and 81 mg aspirin medical therapy.

Four months post-infection, the patient again experienced multiple episodes of left hemiparesis, dysarthria, and gait ataxia. Clinical evaluation demonstrated a concern for underlying vasculitis. Digital subtraction angiography (DSA) at this time demonstrated stable bilateral ICA FMD as well as marked progression of stenosis in the right ICA and MCA seen 2 months earlier on CTA (Fig. 2B). The distal right ICA and proximal M1 segment demonstrated diffuse stenosis with irregular beading of the vessels and delayed cortical filling, no filling of the right A1 segment, collateralization from the right posterior circulation, and increased caliber of lenticulostriate vessels. The findings represented Suzuki stage III moyamoya changes (Fig. 3A-C). MRI performed at this time demonstrated multiple acute infarcts in the right frontal, parietal, and temporal lobes along with diffuse FLuid-Attenuated-Inversion-Recovery (FLAIR) hyperintensity within the right hemisphere.

Five months post-infection, vessel wall imaging (VWI), hemodynamic imaging, and magnetic resonance angiography (MRA) were performed to assess hemodynamic compromise (Table 1). Anatomic MRI performed at this time revealed the evolution of the subacute right hemispheric infarcts (Fig. 4A,C). CBF-weighted MRI demonstrated decreased right-sided CBF (41.3 ml/100g/min) compared to the contralateral hemisphere (46.6 ml/100g/min) with endovascular artifact consistent with delayed blood arrival time (Fig. 4G). Cerebrovascular reactivity (CVR)-weighted mapping indicated diffusely impaired right-sided reserve capacity with a relative reactivity 4.6-fold lower than the left MCA territory (Fig. 4E). Whole-brain oxygen extraction fraction (OEF) was observed to be 0.42, higher than what has been previously found for healthy controls using an identical protocol (interquartile range=0.29-0.38) and consistent with oxygen demand exceeding oxygen delivery.[8] Intracranial VWI demonstrated thickening of the right MCA (maximum wall thickness=2.6 mm) compared to the contralateral MCA (maximum wall thickness=0.8 mm) (Fig. 5A,C).

All other typical ischemic stroke evaluations were negative, including echocardiogram, cholesterol panel, and infectious/inflammatory laboratory studies (erythrocyte sedimentation rate and C-reactive protein). Lumbar puncture was planned but deferred following angiographic findings. She was prescribed aspirin and cilostazol (50 mg, twice daily), and surgical revascularization was offered as the length of time from the initial inciting inflammatory event implied that the anatomic changes would be unlikely to reverse with isolated medical therapy.

Surgical management

Due to the progressive nature of the patient's symptoms and imaging findings, the moyamoya configuration of vasculopathy, and the failure of medical therapy, surgical revascularization was pursued in the form of a direct STA-MCA bypass six months after initial clinical presentation. A direct bypass was chosen due to the robust size of the parietal STA branch (diameter=1.6 mm), rapid symptom progression, and age. A standard surgical preparation was undertaken with an initial distal-to-proximal dissection of the STA, vessel preparation, and underlying craniotomy. The frontal STA branch was not utilized as it was diminutive and far anterior past the hairline, making it a poor candidate for inclusion cosmetically; furthermore, the posterior STA branch was directly overlying the affected area

demonstrated by FLAIR imaging. Once a suitable cortical MCA branch was prepared, an end-to-side anastomosis was performed with a fish-mouthed STA graft and interrupted 9-0 nylon sutures. Intra-operative indocyanine green video-angiography was performed demonstrating good patency of the anastomosis. The residual peri-vascular cuff was then sutured to the exposed pia with 9-0 nylon sutures to provide additional pial synangiosis. No intra-operative or post-operative complications were observed.

Follow-up

The patient tolerated surgery well and was maintained on aspirin and cilostazol. On last follow-up examination (one year post-operatively) the patient demonstrated a fully intact neurological examination with no residual symptoms. The patient resumed all pre-stroke activities with a modified Rankin Score=0.

DSA and anatomical and hemodynamic MRI were performed one year post-operatively. DSA revealed persistent stenosis in the distal ICA and proximal MCA, but improved quality of cortical filling (Fig. 3D-F). The STA graft demonstrated preserved patency and excellent filling in both directions at the anastomosis site into the posterior and inferior MCA cortical territories. Filling is seen from the anastomosis into the more superior MCA territories with less robustness, likely due to improved proximal MCA filling as the HZO resolved and supply from the anastomosis was less critical. Anatomical MRI showed the evolution of white matter chronic infarcts, but no new infarcts were observed (Fig. 4B,D). Hemodynamic CBF-weighted imaging revealed an increase in CBF to 70.7 ml/100g/min in the MCA territory of the right hemisphere (Fig. 4H). CVR analysis revealed an increase in the post-operative right hemisphere reactivity, with a relative reactivity 1.3-fold lower than the contralateral MCA territory, indicating more symmetric reactivity than present prior to surgery. (Fig. 4F). Whole-brain OEF decreased post-surgery to 0.38. Finally, VWI revealed reduction in the thickness of the right MCA (maximum wall thickness=2.2 mm); however, wall thickness remained elevated compared to the contralateral MCA vessel wall (Fig. 5B,D).

Discussion

We present a case of direct surgical revascularization in a patient with progressive infarcts and vasculopathy following HZO. While varicella zoster vasculopathy is a well-described[6] cause of stroke, medical management is considered standard-of-care, and revascularization of HZO-induced vasculopathy has not been reported. In this case, treatment of HZO-induced vasculopathy, for which surgery is not typically considered, in a moyamoya pattern with a surgical bypass resulted in an excellent clinical outcome. At most medical centers, such patients are managed through the Neurology services generally without neurosurgery consultation, but this work highlights that such consultations may be warranted when aggressive disease is present or patients respond sub-optimally to medical therapy. As atypical presentations of moyamoya vasculopathy are being observed more frequently, particularly in the United States,[9] increased awareness is critical for appropriate treatment. While medical management is the best course of treatment for HZO-induced vasculopathy,[10]

surgical revascularization may be considered for cases in which there is rapid progression of symptomatic stenoses and medical therapy is not successful.

In this case, conventional imaging demonstrated the progressive nature of the symptomatic stenoses in the months following infection and before surgical intervention. Hemodynamic imaging provided additional information for monitoring the functional status of the brain before and after surgery. CBF-weighted imaging demonstrated increased right-sided blood flow post-revascularization. CVR-weighted imaging showed improvements in the right hemisphere following surgery. The increase in CVR is consistent with reductions in autoregulation extent, normalized arteriolar blood volume, and increased reserve capacity. OEF, which reflects the fraction of oxygen consumed to oxygen delivered and has been suggested as an indicator of disease severity[8,11], decreased following revascularization, indicating improvements in oxygen delivery. Finally, VWI, which has in recent studies been shown to be discriminatory for determining etiology of vasculopathy,[12-14] was performed which aided in diagnosis of inflammatory vasculopathy likely due to HZO.

In cases of patients with vasculitis who do not respond to more conservative medical management, intracranial angioplasty has been performed; however, it has been shown to have no long-term benefit, as occlusion ensued in all cases post-intervention.[15] Furthermore, angioplasty would not be a viable option in the setting of diffuse stenoses, such as in the case of moyamoya configuration. As the patient was asymptomatic prior to HZO infection, no imaging was performed prior to the onset of neurological symptoms in this case. As such, we cannot definitely conclude that the moyamoya was secondary to the HZO infection, although given the lack of symptoms prior to infection this is logical. This is also consistent with the progression from mild right A1 stenosis and a small (4mm) region of diffusion restriction in the right parietal hemisphere two months post-infection to significant, flow-limiting stenosis of the right distal ICA and M1 and multiple areas of restricted diffusion in the right frontal, parietal, and temporal lobes four months post-infection, suggesting HZO-induced vasculopathy. The time to presentation with infarcts is consistent with literature on vasculopathy post-infection.[4,5] Finally, additional cases of HZO-induced progressive vasculopathy will be needed to fully understand the utility of revascularization in this group of patients for whom medical management has failed; however, this case suggests that surgical revascularization should be considered in such patients with aggressive disease.

Conclusion

We present a case of progressive, symptomatic stenoses in a moyamoya configuration following HZO as well as the first reported description of the cerebral hemodynamic impact that revascularization surgery can provide in such a setting. This case report highlights the utility of combined evaluation of similar cases of progressive disease with hemodynamic imaging and demonstrates the benefits of surgical bypass in such patients responding inadequately to medical therapy. While moyamoya is a common condition, this case presents an uncommon cause and novel treatment and emphasizes the importance of multi-modal evaluation.

Acknowledgments

This work was supported by the National Institutes of Health and the National Institute of Neurological Disorders and Stroke (5R01NS078828 and 1R01NS097763)

References

1. Cockburn DM, Douglas IS. Herpes zoster opthalmicus. Clin Exp Optom. 2000; 83(2):59–64. [PubMed: 12472455]
2. Hilt DC, Buchholz D, Krumholz A, Weiss H, Wolinsky JS. Herpes zoster ophthalmicus and delayed contralateral hemiparesis caused by cerebral angiitis: diagnosis and management approaches. Ann Neurol. 1983; 14(5):543–553. [PubMed: 6606387]
3. Ueno M, Oka A, Koeda T, Okamoto R, Takeshita K. Unilateral occlusion of the middle cerebral artery after varicella-zoster virus infection. Brain Dev. 2002; 24(2):106–108. [PubMed: 11891103]
4. Bourdette DN, Rosenberg NL, Yatsu FM. Herpes zoster ophthalmicus and delayed ipsilateral cerebral infarction. Neurology. 1983; 33(11):1428–1432. [PubMed: 6605495]
5. Nagel MA, Cohrs RJ, Mahalingam R, et al. The varicella zoster virus vasculopathies: clinical, CSF, imaging, and virologic features. Neurology. 2008; 70(11):853–860. [PubMed: 18332343]
6. Nagel MA, Jones D, Wyborny A. Varicella zoster virus vasculopathy: The expanding clinical spectrum and pathogenesis. J Neuroimmunol. 2017; 308:112–117. [PubMed: 28335992]
7. Arias EJ, Derdeyn CP, Dacey RG, Zipfel GJ. Advances and Surgical Considerations in the Treatment of Moyamoya Disease. Neurosurgery. 2014; 74(suppl_1):S116–S125. [PubMed: 24402480]
8. Watchmaker JM, Juttukonda MR, Davis LT, et al. Hemodynamic mechanisms underlying elevated oxygen extraction fraction (OEF) in moyamoya and sickle cell anemia patients. J Cereb Blood Flow Metab. 2016 271678X16682509.
9. Hallemeier CL, Rich KM, Grubb RL Jr, et al. Clinical features and outcome in North American adults with moyamoya phenomenon. Stroke. 2006; 37(6):1490–1496. [PubMed: 16645133]
10. Amlie-Lefond C, Gilden D. Varicella Zoster Virus: A Common Cause of Stroke in Children and Adults. J Stroke Cerebrovasc Dis. 2016; 25(7):1561–1569. [PubMed: 27138380]
11. Iwama T, Akiyama Y, Morimoto M, Kojima A, Hayashida K. Comparison of positron emission tomography study results of cerebral hemodynamics in patients with bleeding-and ischemic-type moyamoya disease. Neurosurg Focus. 1998; 5(5):e3.
12. Swartz RH, Bhuta SS, Farb RI, et al. Intracranial arterial wall imaging using high-resolution 3-tesla contrast-enhanced MRI. Neurology. 2009; 72(7):627–634. [PubMed: 19221296]
13. Mossa-Basha M, de Havenon A, Becker KJ, et al. Added Value of Vessel Wall Magnetic Resonance Imaging in the Differentiation of Moyamoya Vasculopathies in a Non-Asian Cohort. Stroke. 2016; 47(7):1782–1788. [PubMed: 27272486]
14. Cheng-Ching E, Jones S, Hui FK, et al. High-resolution MRI vessel wall imaging in varicella zoster virus vasculopathy. J Neurol Sci. 2015; 351(1-2):168–173. [PubMed: 25732801]
15. McKenzie JD, Wallace RC, Dean BL, Flom RA, Khayata MH. Preliminary results of intracranial angioplasty for vascular stenosis caused by atherosclerosis and vasculitis. AJNR Am J Neuroradiol. 1996; 17(2):263–268. [PubMed: 8938296]
16. Wang J, Alsop DC, Li L, et al. Comparison of quantitative perfusion imaging using arterial spin labeling at 1.5 and 4.0 Tesla. Magn Reson Med. 2002; 48(2):242–254. [PubMed: 12210932]
17. Donahue MJ, Dethrage LM, Faraco CC, et al. Routine clinical evaluation of cerebrovascular reserve capacity using carbogen in patients with intracranial stenosis. Stroke. 2014; 45(8):2335–2341. [PubMed: 24938845]
18. Lu H, Ge Y. Quantitative evaluation of oxygenation in venous vessels using T2-Relaxation-Under-Spin-Tagging MRI. Magn Reson Med. 2008; 60(2):357–363. [PubMed: 18666116]

Abbreviations

CBF	Cerebral blood flow
CTA	Computed tomography angiography
CVR	Cerebrovascular reactivity
DSA	Digital subtraction angiography
EPI	Echo Planar Imaging
FLAIR	FLuid-Attenuated-Inversion-Recovery
FMD	Fibromuscular dysplasia
HZO	Herpes zoster ophthalmicus
ICA	Internal carotid artery
MCA	Middle cerebral artery
MPRAGE	Magnetization-Prepared Rapid Gradient-Echo
MRA	Magnetic resonance angiography
MRI	Magnetic resonance imaging
OEF	Oxygen extraction fraction
STA	Superficial temporal artery
TE	Echo Time
TI	Inversion Time
TSE	Turbo Spin Echo
TR	Repetition Time
VWI	Vessel

Highlights

- Herpes zoster can lead to progressive vasculopathy with moyamoya collaterals
- Such progressive vasculopathy may not respond to standard medical management
- Surgical bypass can improve cerebral hemodynamics and symptoms in such patients
- Revascularization should be considered for aggressive herpes zoster vasculopathy

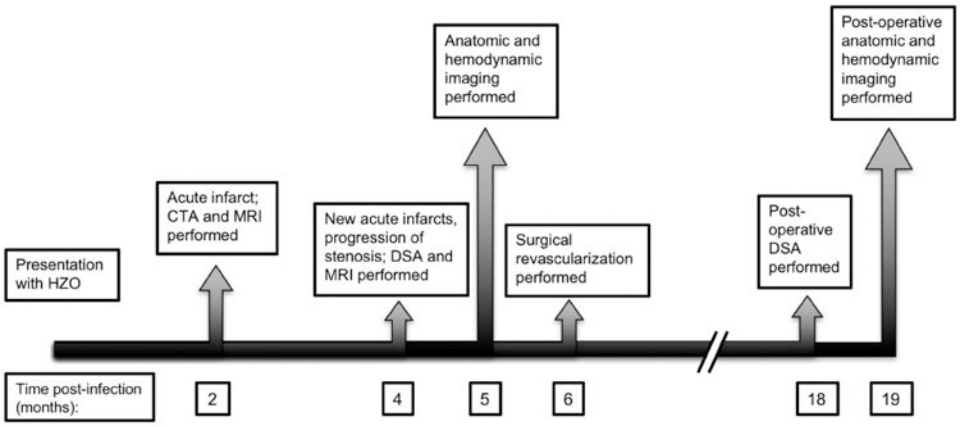

Figure 1.

Timeline of clinical history, including computed tomography angiography (CTA), digital subtraction angiography (DSA), and magnetic resonance imaging (MRI) at multiple time points.

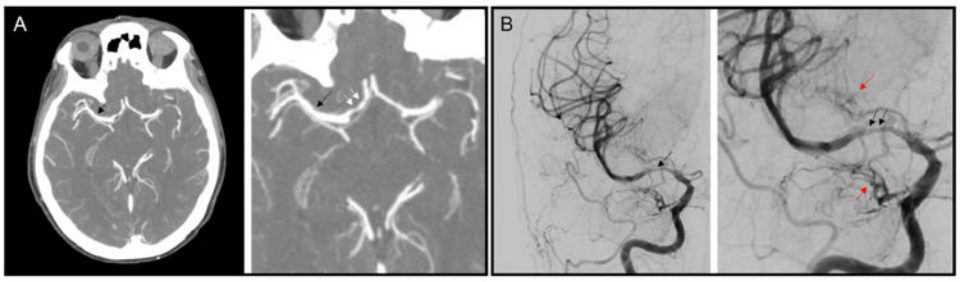

Figure 2.

Stenosis progression before surgical revascularization. (A) CT angiography performed 2 months post-infection showing mild focal stenosis of the right M1 segment (black arrow). Moderate multi-focal stenosis is seen in the A1 segment (white arrows). (B) Digital subtraction angiography performed 4 months post-infection showing distal ICA stenosis, long segment moderate to severe stenosis of the M1 segment (black arrows), and no filling of the A1 segment. Regional moyamoya-type collateralization is appreciated (red arrows).

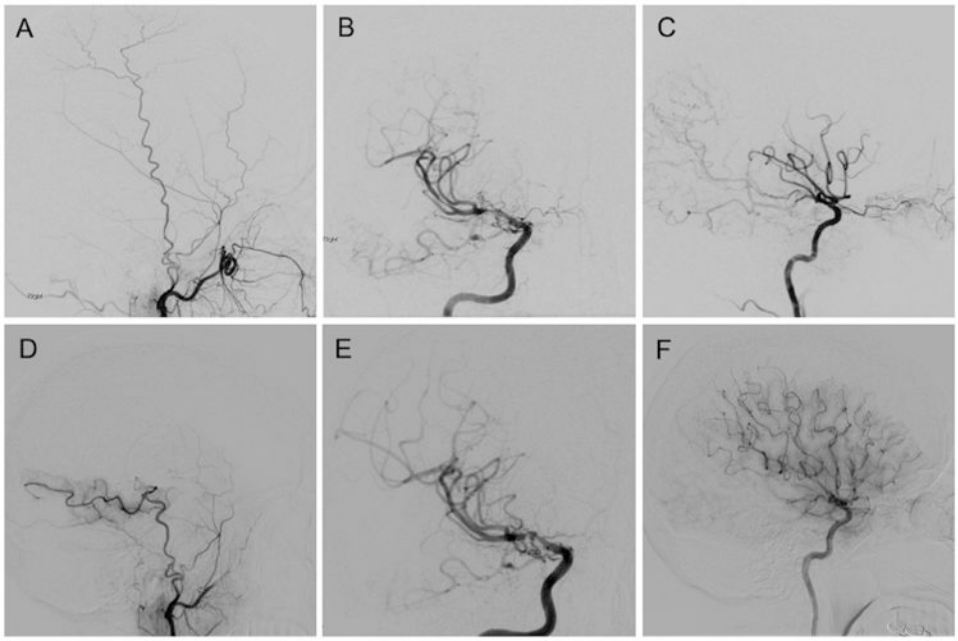

Figure 3.

Digital subtraction angiography (DSA) of the right external carotid artery (ECA) and internal carotid artery (ICA) performed pre-operatively **(A-C)** and one year post-operatively **(D-E)**. Note the degree of stenosis in the ICA and MCA **(B)** and the paucity of filling of the MCA parenchyma **(C)** before surgery. Post-operatively, the patency of the STA graft into the posterior inferior MCA territory is seen **(D)**. Improvement of stenosis in the ICA and MCA **(E)** as well as improved filling of the MCA parenchyma **(F)** are also noted post-operatively.

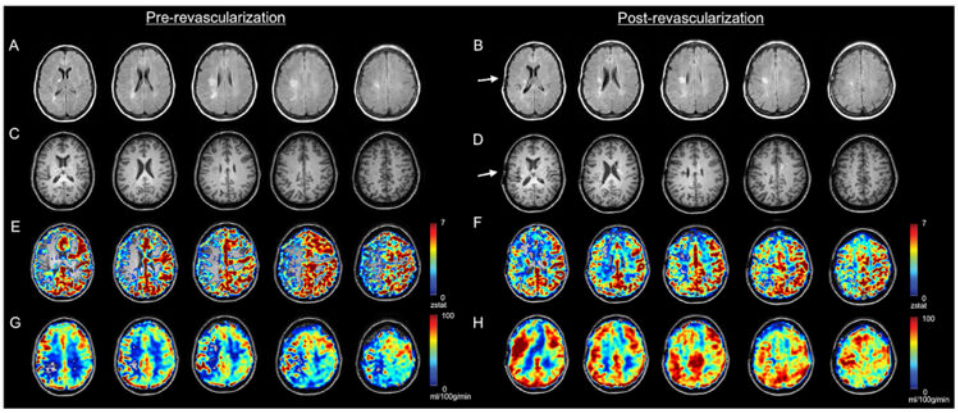

Figure 4.

Anatomical and hemodynamic imaging performed before surgical revascularization and one year after surgical revascularization. (**A)** Axial slices from T_2-weighted FLAIR MRI reveal multiple infarcts in the right hemisphere following infection. **(B)** T_2-weighted FLAIR MRI after surgical revascularization reveals the evolution of the same infarcts, but suggests no new infarction. Arrows denote the site of surgical revascularization. Axial slices from T_1-weighted MRI demonstrate the same infarcts before **(C)** and after **(D)** surgical revascularization. Axial slices from CVR-weighted hemodynamic imaging show decreased right-sided reactivity pre-surgery **(E)** and improved right-sided reactivity post-surgery **(F)**. Axial slices from CBF-weighted imaging show decreased blood flow in the right MCA territory pre-surgery **(G)** and increased CBF in the right hemisphere post-surgery **(H)**.

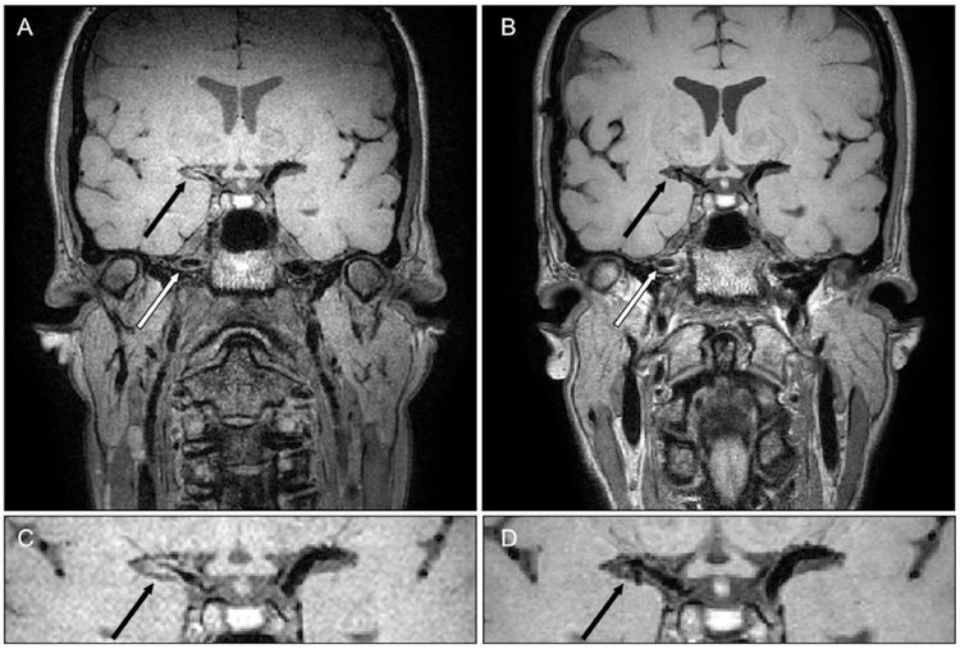

Figure 5.

(A) Vessel wall imaging (VWI) performed five-months post-infection demonstrates severe concentric vessel wall thickening of the right distal cervical ICA (white arrow) and the right ICA terminus and proximal MCA (black arrow). (**B)** VWI performed one year post-surgery reveals persistent cervical ICA wall thickening (white arrow) on the right compared to the left. **(C)** Magnified coronal slice of the MCA demonstrates the intracranial wall thickening (black arrow). **(D)** Improvement is seen at 14-month follow-up (black arrow).

Table 1
Imaging and angiographic techniques and corresponding physiological parameters

Measurement (units)	Method	Relevant parameters
Angiographic (Allura Xper, Philips Medical Systems, Best, The Netherlands)		
Lumen diameter (percent stenosed)	Digital subtraction angiography	Catheterization and injection of the right ICA, right ECA, left vertebral artery, and left common carotid artery.
Anatomical (3.0T Achieva, Philips Medical Systems, Best, The Netherlands)		
Infarcts (count and volume)	FLAIR	Spatial resolution=0.4×0.3×5.0 mm^3; TR/TE/TI=11000/120/2800 ms; 2D spin echo EPI.
Tissue structure	T1-weighted	Spatial resolution=1.0×1.0×1.0 mm^3; TR/TE=9.0/4.6 ms; 3D MPRAGE.
Vessel wall thickness (mm)	3D turbo-spin-echo MRI	Spatial resolution=0.6×0.5×0.5 mm^3; variable refocusing angle=40-120deg; TR/TE=1500/38.5 ms; TSE-factor=56; duration=6 min 51 s.
Hemodynamic (3.0T Achieva, Philips Medical Systems, Best, The Netherlands)		
CBF (ml/100g/min)	Pseudo-continuous arterial spin labeling (pCASL)	Spatial resolution=3.5×3.4×5.0 mm^3; duration=4 min 20 s; TR/TE/post-labeling delay = 4000/13/1800 ms; 2D gradient echo EPI. CBF was quantified using a two-compartment kinetic model.[16]
CVR (Z-statistic)	Hypercapnic blood oxygenation level-dependent (BOLD) MRI	Statistical measure of how well each voxel responds to hypercapnic stimulus without correcting for reactivity timing delays: z-statistic between stimulus regressor and voxel time course. Protocol is identical to previously described.[17] Two 3-minute blocks of hypercapnia were administered interleaved with room air. BOLD-weighted, spatial resolution=3.0×3.0×3.5 mm^3; TR/TE=2000/35 ms; duration=12 min 10s; 2D gradient echo EPI.
OEF (unitless)	TRUST MRI	Ratio of oxygen consumed to oxygen delivered. T2-relaxation-under-spin-tagging (TRUST) using previously described parameters.[18] Four effective echo times: 0, 40, 80, and 160 ms. Image acquired 20 mm superior to confluence of sinuses. Duration=1 min 12 s.